Materials Advances

ROYAL SOCIETY OF CHEMISTRY

PAPER

View Article Online
View Journal | View Issue

Cite this: *Mater. Adv.*, 2023, 4, 6271

Concentration-dependent emission from low molecular weight benzoyl pyrazinium salts†

Ryan P. Brisbin,‡[a] Arya Karappilly Rajan,[b] Md. Imran Khan,[b] Pravien S. Rajaram,[a] Karen M. Russell,[a] Sayantani Ghosh*[b] and Ryan D. Baxter*[a]

Received 15th June 2023,
Accepted 22nd October 2023

DOI: 10.1039/d3ma00302g

rsc.li/materials-advances

Low molecular weight benzoyl pyrazinium (BP) salts with different structures have been synthesized and analyzed for their photophysical properties. All BP salts studied were found to be optically active in the visible region with structural variations influencing their emission energies. Further, a strong concentration dependence was observed for each BP, whereby dilute solutions had higher emission energies, greater emission intensities and increased recombination lifetimes. NMR data shows that rates of molecular diffusion are slower at higher concentrations suggesting the formation of solution-phase aggregates is responsible for concentration-dependent photophysical behavior, with internal quenching affecting the observed emission at high concentrations. Reliable correlations between energies of excitation and emission were also demonstrated, suggesting that photophysical properties depend on a combination of chemical structure, concentration, and energy of photoexcitation. The BP salts discussed here represent a promising class of easily synthesized low molecular weight organic molecules with tunable emission properties.

Luminescent materials have important applications in many diverse fields of science, from biomedical sensing to electronic displays.[1–3] The utility of luminescent materials often depends on the specific application, but there is a consistent drive to develop new materials that are cost-effective, sustainable, and have tunable emission properties.[2–7] In this context, organic molecules show promise as a potentially robust class of luminescent materials as synthetic advances continuously increase the number and variety of structures that can be targeted. The utility of organic light-emitting diodes (OLEDs) has been established by the electronics industry, and recent advances have produced purely organic materials capable of narrowband emissions of high purity light.[1,8–10] To minimize vibronic coupling and structural relaxation in photoexcited states, many frameworks are designed as large, rigid structures with multiple conjugated or fused aromatic systems.[11–13] Such structures are intentionally designed to produce desired photophysical properties, but are difficult to fine-tune *via* straightforward synthetic modifications. Through our work developing organic-based electrolyte salts we have identified a class of molecules, benzoyl pyrazinium (BP) salts, with interesting photophysical properties (Fig. 1A). Routine spectroscopic characterization showed the benzoyl pyrazinium salts to be strongly emissive in the visible range (Fig. 1B) when excited with an ultraviolet (UV) source. In addition, the general structure of the BP salt is easily synthesized in three steps from commercial materials (Fig. 1C). Although these structures proved to be inefficient organic electrolytes, we became interested in further exploring their photophysical behavior of BPs to determine their potential value as luminescent materials.

We utilized a previously developed method (a variant of the Minisci reaction to functionalize heteroarenes under mild conditions) to target BP salts as supporting electrolytes for electrocatalysis.[14] During routine characterization the BP salts showed strong absorption in the UV region, with accompanying emissions of visible light strong enough to be observed with the naked eye (Fig. 1B). Further investigation into the photophysical properties of the BP salts revealed that emission depended on several factors that could be experimentally controlled and tuned to produce varied emissions in a predictable manner.

Three BP tetrafluoroborate salts were initially synthesized with variation of the acetophenone starting material at the 4-position (Fig. 2, top). The photoluminescence (PL) emission shown in Fig. 2 (bottom) demonstrated the extent to which the electronic nature of the benzoyl group affected emission in 10 mM acetonitrile solutions. Electron-withdrawing substituents (**F-BF$_4$**) produced BP salts that emit light with the lowest energy

[a] *Department of Chemistry and Biochemistry, University of California, 5200 N. Lake Road, Merced, California 95343, USA. E-mail: rbaxter@ucmerced.edu*
[b] *Department of Physics, University of California, 5200 N. Lake Road, Merced, California 95343, USA. E-mail: sghosh@ucmerced.edu*

† Electronic supplementary information (ESI) available: The following files are available free of charge. General synthetic procedures, spectral/analytical data, DOSY-NMR spectra (PDF). CCDC 2300176. For ESI and crystallographic data in CIF or other electronic format see DOI: https://doi.org/10.1039/d3ma00302g

‡ These authors contributed equally.

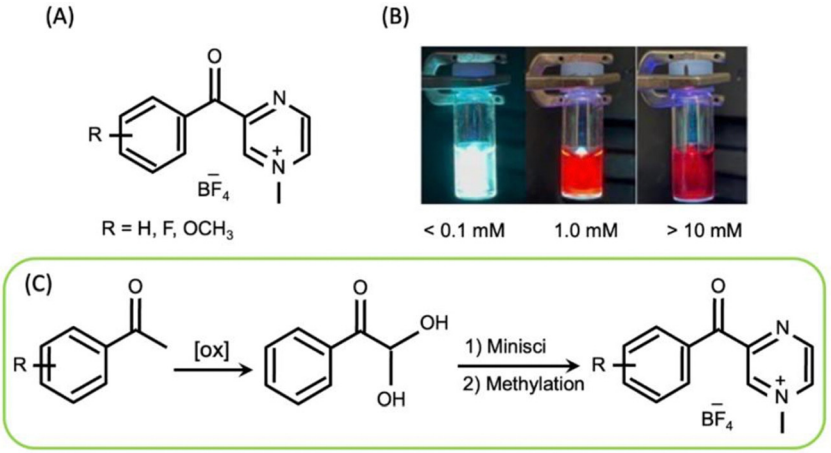

Fig. 1 (A) Chemical structure and (B) luminescence of BP salts. (C) Synthesis scheme of BP salts from acetophenones.

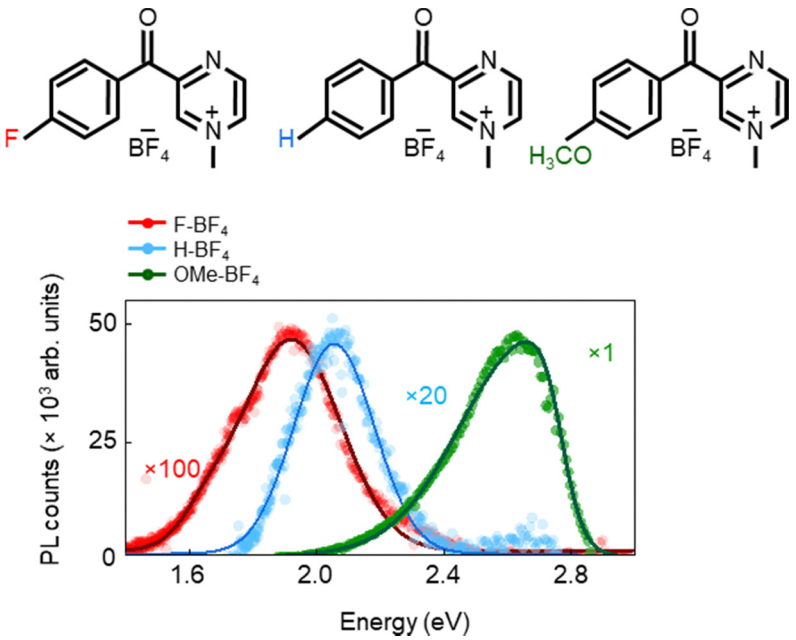

Fig. 2 (top) Chemical structures and (bottom) photoluminescence (PL) emission of 10 mM solutions of BP salts in acetonitrile. Excitation energy tuned to 2.88 eV (430 nm). Counts for **F-BF$_4$** and **H-BF$_4$** have been magnified for visual purposes.

and intensity. As the BP salts were made to possess more electron-density through the benzoyl group (**H-BF$_4$**), the emission blue-shifted while producing higher intensity light. The trend continued with the most electron-rich benzoyl group studied (**OCH$_3$-BF$_4$**), producing emission of the greatest intensity and highest energy. A possible explanation for the variation in emission data is an intrinsic difference in photoluminescent quantum yield resulting from the compositional changes between the molecules.[11] Alternatively, differing degrees of intermolecular charge transfer may cause emission to quench by allowing additional non-radiative pathways. To clarify the underlying cause of the wide variation in emission energy and intensity seen in Fig. 2, we explored **H-BF$_4$** solutions at different concentrations in acetonitrile in Fig. 3.

Absorption and PL spectra in Fig. 3A confirmed a strong concentration dependence for solutions of BPs in acetonitrile. Peak emission energy varied from 2.61 eV at 0.1 mM concentration to 1.98 eV at 100 mM, while also showing a decrease in emission intensity with increasing concentration. The absorption band demonstrated a similar spectral shift (Fig. S1, ESI†). Spectral red-shift in discrete fluorophores is commonly caused by energy transfer (ET), where high energy photons emitted by 'donors' are absorbed by 'acceptors' with lower energy gaps and re-emitted, which cause the final emission to occur at longer wavelengths, or at lower energies. The most well-known mechanism is Förster Resonant Energy Transfer (FRET) resulting from dipolar coupling of individual fluorophores (molecules, quantum dots, *etc.*) in an ensemble.[12] However, ET between fluorophores

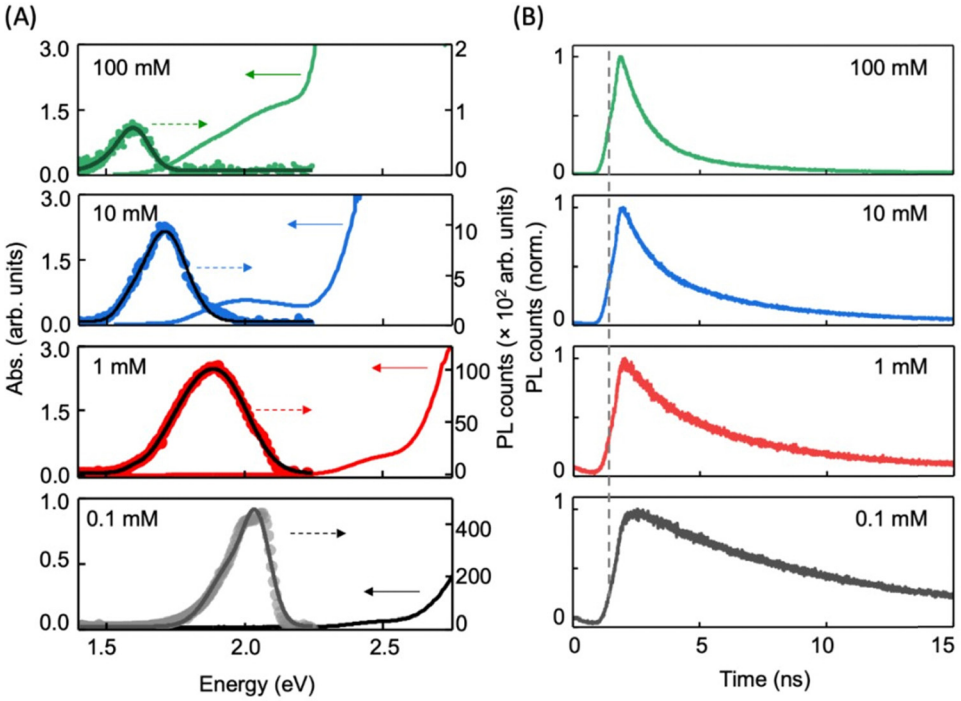

Fig. 3 (A) Absorption (solid arrows) and PL emission (dashed arrows) spectra, and (B) recombination lifetimes for **H-BF$_4$** solution at different concentrations. Both absorption and PL blue-shift with decreasing concentration, accompanied by increasing lifetime. The dashed line in (B) highlights a gradual change in the rise time.

in solution is rare due to the large inter-particle separation. Further, energy transfer induced emission redshift is typically not accompanied by a concurrent shift of the absorption band, as observed here. The changes in PL and absorption with concentration suggest the formation of coupled hierarchical molecular clusters (aggregates) whose inherent energy transitions are smaller. Analogous absorption and PL data using methanol as solvent did not show concentration-dependent changes in emission (Fig. S2, ESI†), with identical energies of emission observed across the range of concentrations studies. To us, this suggested that intermolecular interactions were affecting absorbance and emission behavior, with greater intermolecular interactions occurring in solutions of higher concentration.

To understand the effect of concentration more fully on charge or energy transfer dynamics, time resolved photoluminescent (TRPL) spectroscopy was obtained for all the concentrations of **H-BF$_4$** (Fig. 3B). The PL counts decreased exponentially with time for all the concentrations, but the decay was faster as concentration increased. Again, as a point of comparison, ET processes typically have longer recombination lifetimes (slower decay rates) associated with the 'acceptors' to which energy is transferred and whose emission is at lower energies.

While the data in Fig. 3 clearly show that emission behavior is concentration-dependent for **H-BF$_4$**, a direct comparison of these data to **F-BF$_4$** and **OCH$_3$-BF$_4$** provides insight into the general PL behavior for BP salts. Fig. 4A confirms that peak energy decreased at higher concentrations for all species, although the magnitude of this effect depends on the structural identity of the BP salt. Interestingly, similar energies of emission are observed at low concentration, where intermolecular charge-transfer is minimized, with divergence setting in as concentration increases. The similarities in variation of PL intensity and recombination lifetimes with concentration are also confirmed in all BP salts, shown in Fig. 4B and C, respectively.

The lifetimes plotted in Fig. 4C were extracted from fitting TRPL curves such as those in Fig. 3B with a biexponential $I_{pl} = A_1e^{-t/\tau_1} + A_2e^{-t/\tau_2}$ function, where I_{pl} is the PL emission intensity. The average lifetime was calculated using $\tau = (A_1\tau_1^2 + A_2\tau_2^2)/(A_1\tau_1 + A_2\tau_2)$.[15] All BPs exhibited similar trends in which the more dilute the sample, the longer the lifetime. The number of non-radiative decay pathways appears to increase with concentration,[8,20] possibly as a result of increased efficiency of intramolecular charge transfer.[16–21] Further dilution of the **H-BF$_4$** sample to 0.01 mM shows a single exponential decay with time, suggesting minimal presence of aggregates at this and lower concentrations (Fig. S3, ESI†).

Given the emergence of relaxation routes with increasing concentration, Fig. 5 focuses on solutions of **H-BF$_4$** (>1 mM) with the goal of understanding how increasing photoexcitation energy tune the emission properties. Fig. 5A and B map the PL emission spectra for the 10 mM and 100 mM solutions as excitation energy was changed. Fig. 5C summarizes emission energy varying with excitation energy at 1 mM, 10 mM, and 100 mM solutions. For all, the emission energy blue shifted with increasing excitation energy. This is expected, as at higher excitation energy the smaller aggregates absorb more strongly and contribute more to the total PL intensity. Interestingly, with increasing concentration, the range of excitation where emission

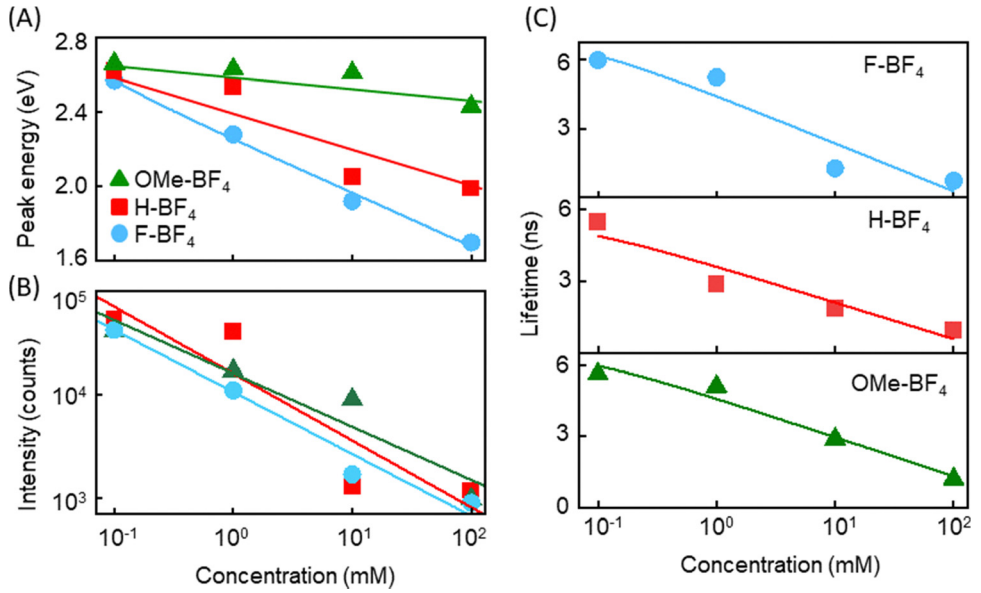

Fig. 4 Variation of (A) peak emission energy, (B) emission intensity and (C) recombination lifetime with concentration for all BPs.

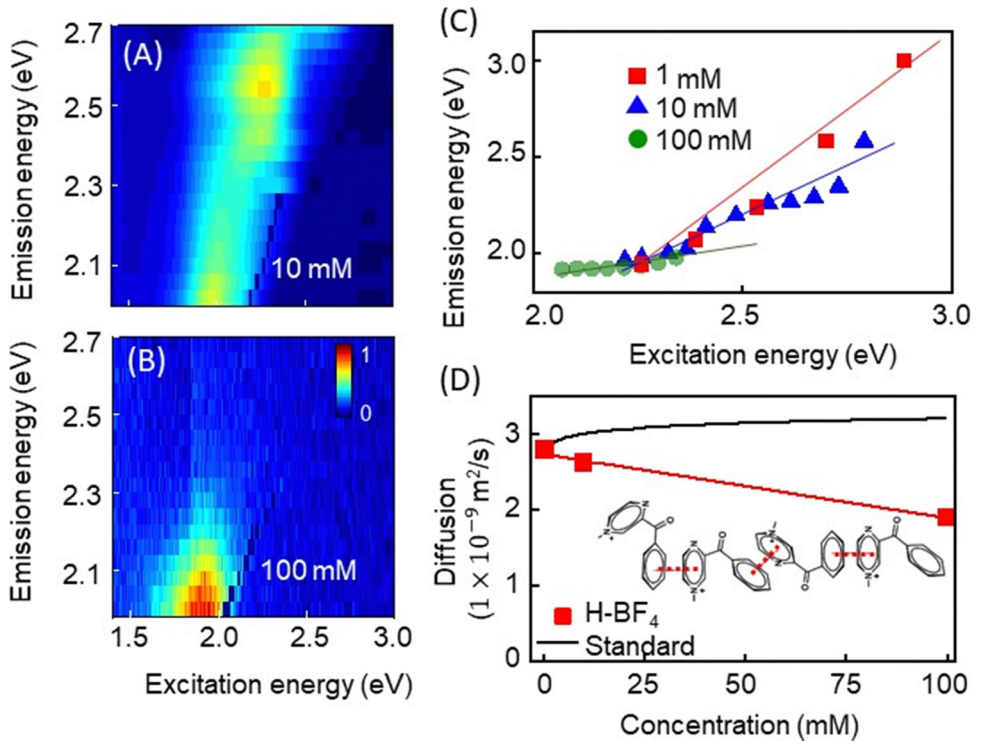

Fig. 5 (A) and (B) Color map of PL intensity spectra of 10 mM and 100 mM concentations of **H-BF$_4$** solutions taken at different excitation energies. (C) Peak emission energy exhibits blue shift with increasing excitation energy. Lines are guides to the eye. (D) Decreasing rates of molecular diffusion with increasing **H-BF$_4$** concentration (red) compared to an internal standard (black).

is observed shortened. For 100 mM concentration, no emission is observed once excitation energy exceeds 2.3 eV. As Fig. 3A shows, clearly the sample absorbs beyond this, but the emission is quenched.

The presence of a large population of larger aggregates with smaller emission energies could facilitate energy transfer from the smaller, high-energy emitting entities, resulting in no PL emission at high energies. Dynamic light scattering (DLS) was attempted to verify the presence the aggregated species, but data acquisition was not effective; at the higher concentrations most likely to exhibit aggregation behavior, fluorescence and absorption prevented any meaningful results, whereas at

concentrations low enough for DLS to work, no aggregation (or any signal different from the background solvent) was observed. To further explore the possibility of solution-phase aggregates, diffusion-ordered NMR spectroscopy (DOSY) was performed.[22] As shown in Fig. 5D, the translational self-diffusion coefficient of **H-BF$_4$** (red line) varied with solution concentration compared to an internal standard (black curve). Slower diffusion at high concentration, independent of changes in solubility or solution viscosity, suggests the presence of higher-ordered aggregate species.[23] The formation of aggregates is expected to dramatically reduce quantum yield due to the number of non-radiative decay pathways for depopulation of the excited state. Concentration-depended photoluminescence quantum yield (PLQY) measurements showed that PLQY decreases with increasing concentration, with samples of low concentration (0.1 mM) producing the highest observed quantum yield of 60% (Table S1, ESI†). One possibility for aggregate structural arrangement is shown in Fig. 5D, whereby electrostatic interactions between neighboring pyrazinium and benzoyl groups associate *via* π-stacking. Single-crystal X-ray diffraction reveals intermolecular spacing of 3.4 angstroms in the unit cell, a value that is consistent with electrostatic interactions of π-systems.[24]

The combined data discussed above demonstrate that low molecular weight benzoyl pyrazinium structures are an attractive platform on which to build tunable photophysical organic materials. All molecules studied demonstrate solution phase emission in the visible range, with some variation in emission energy and intensity depending on chemical structure. Concentration- dependent changes in emission were more pronounced, with low concentrations producing emissions with the greatest energy and longest lifetime. DOSY data suggest that solution-phase aggregation is responsible for this behavior, with internal quenching affecting the observed emission at high concentrations. A reliable correlation between energies of excitation and emission was also demonstrated, suggesting that photophysical properties depend on a combination of chemical structure, concentration, and energy of photoexcitation.

Conflicts of interest

The authors declare no competing financial interests.

Acknowledgements

This material is based upon work supported by the National Science Foundation under Grant No. NSF-CAREER 1752821 (R. D. B) and NSF-CREST HRD-1547848 (S. G., R. P. B.).

References

1 J. Ma, T. Shu, Y. Sun, X. Zhou, C. Ren, L. Su and X. Zhang, Luminescent Covalent Organic Frameworks for Biosensing and Bioimaging Applications, *Small*, 2021, **18**(3), 2103516, DOI: 10.1002/smll.202103516.

2 X. Ren, X. Zhang, H. Xie, J. Cai, C. Wang, E. Chen, S. Xu, Y. Ye, J. Sun, Q. Yan and T. Guo, Perovskite Quantum Dots for Emerging Displays: Recent Progress and Perspectives, *Nanomaterials*, 2022, **12**(13), 2243, DOI: 10.3390/nano12132243.

3 C. Gao, Y. Wang, Z. Ye, Z. Lin, X. Ma and Q. He, Biomedical Micro-/Nanomotors: From Overcoming Biological Barriers to in Vivo Imaging., *Adv. Mater.*, 2020, **33**(6), 2000512, DOI: 10.1002/adma.202000512.

4 Y. Wang, H. Wu, W. Hu and J. F. Stoddart, Color-Tunable Supramolecular Luminescent Materials, *Adv. Mater.*, 2022, **34**(22), e2105405, DOI: 10.1002/adma.202105405.

5 P. Rawat, P. Nain, S. Sharma, P. K. Sharma, V. Malik, S. Majumder, V. P. Verma, V. Rawat and J. S. Rhyee, An Overview of Synthetic Methods and Applications of Photoluminescence Properties of Carbon Quantum Dots, *Luminescence*, 2022, **38**(7), 845–866, DOI: 10.1002/bio.4255.

6 K. Kumar Gangu, S. Maddila and S. B. Jonnalagadda, The Pioneering Role of Metal–Organic Framework-5 in Ever-Growing Contemporary Applications – a Review., *RSC Adv.*, 2022, **12**(22), 14282–14298, DOI: 10.1039/D2RA01505F.

7 M. Gu, W. Li, L. Jiang and X. Li, Recent Progress of Rare Earth Doped Hydroxyapatite Nanoparticles: Luminescence Properties, Synthesis and Biomedical Applications, *Acta Biomater.*, 2022, **148**, 22–43, DOI: 10.1016/j.actbio.2022.06.006.

8 J. Heo, D. P. Murale, H. Y. Yoon, V. Arun, S. Choi, E. Kim, J. Lee and S. Kim, Recent trends in molecular aggregates: An exploration of biomedicine, *Aggregate*, 2022, **3**, e159–e194, DOI: 10.1002/agt2.159.

9 M. Shimizu and T. Sakurai, Organic Fluorophores That Emit Ultraviolet Light in the Aggregated State, *Aggregate*, 2021, **3**(2), 144, DOI: 10.1002/agt2.144.

10 J. M. Ha, S. H. Hur and A. Pathak, *et al.*, Recent advances in organic luminescent materials with narrowband emission, *NPG Asia Mater.*, 2021, **13**, 53, DOI: 10.1038/s41427-021-00318-8.

11 J. Yang, M. Fang and Z. Li, Organic Luminescent Materials: The Concentration on Aggregates from Aggregation-Induced Emission, *Aggregate*, 2020, **1**(1), 6–18, DOI: 10.1002/agt2.2.

12 C. Grazon, M. Chern, P. Lally, R. C. Baer, A. Fan, S. Lecommandoux, C. Klapperich, A. M. Dennis, J. E. Galagan and M. W. Grinstaff, The Quantum Dot vs. Organic Dye Conundrum for Ratiometric FRET-Based Biosensors: Which One Would You Choose?, *Chem. Sci.*, 2022, **13**(22), 6715–6731, DOI: 10.1039/D1SC06921G.

13 Y. Qin, G. Li, T. Qi and H. Huang, Aromatic Imide/Amide-Based Organic Small-Molecule Emitters for Organic Light-Emitting Diodes, *Mater. Chem. Front.*, 2020, **4**(6), 1554–1568, DOI: 10.1039/D0QM00084A.

14 J. D. Galloway, D. N. Mai and R. D. Baxter, Silver-Catalyzed Minisci Reactions Using Selectfluor as a Mild Oxidant, *Org. Lett.*, 2017, **19**, 5772–5775, DOI: 10.1021/acs.orglett.7b02706.

15 M. D. Bartolo, R. P. Brisbin, S. Ghosh and R. D. Baxter, Impact of Bis (Imino) Pyridine Ligands on Mesoscale Properties of CdSe/ZnS Quantum Dots, *J. Phys. Chem. C*, 2020, **124**(41), 22677–22683, DOI: 10.1021/acs.jpcc.0c06335.

16 Y. Rout, C. Montanari, E. Pasciucco, R. Misra and B. Carlotti, Tuning the Fluorescence and the Intramolecular

Charge Transfer of Phenothiazine Dipolar and Quadrupolar Derivatives by Oxygen Functionalization, *J. Am. Chem. Soc.*, 2021, **143**(26), 9933–9943, DOI: **10.1021/jacs.1c04173**.

17 H. Zhu, M. Li, J. Hu, X. Wang, J. Jie, Q. Guo, C. Chen and A. Xia, Ultrafast Investigation of Intramolecular Charge Transfer and Solvation Dynamics of Tetrahydro[5]-Helicene-Based Imide Derivatives, *Sci. Rep.*, 2016, **6**(March), 1–12, DOI: **10.1038/srep24313**.

18 L. Vachova, V. Novakova, K. Kopecky, M. Miletin and P. Zimcik, Effect of Intramolecular Charge Transfer on Fluorescence and Singlet Oxygen Production of Phthalocyanine Analogues, *Dalton Trans.*, 2012, **41**(38), 11651, DOI: **10.1039/c2dt31403g**.

19 B. Carlotti, G. Consiglio, F. Elisei, C. G. Fortuna, U. Mazzucato and A. Spalletti, Intramolecular Charge Transfer of Push–Pull Pyridinium Salts in the Triplet Manifold, *J. Phys. Chem. A*, 2014, **118**(36), 7782–7787, DOI: **10.1021/jp504963v**.

20 S. Sasaki, G. P. C. Drummen and G. I. Konishi, Recent Advances in Twisted Intramolecular Charge Transfer (TICT) Fluorescence and Related Phenomena in Materials Chemistry, *J. Mater. Chem. C*, 2016, **4**(14), 2731–2743, DOI: **10.1039/c5tc03933a**.

21 A. Cesaretti, C. Bonaccorso, F. Elisei, C. G. Fortuna, L. Mencaroni and A. Spalletti, Photoinduced Intramolecular Charge Transfer and Hyperpolarizability Coefficient in Push–Pull Pyridinium Salts with Increasing Strength of the Acceptor Group, *ChemPlusChem*, 2018, **83**(11), 1021–1031, DOI: **10.1002/cplu.201800393**.

22 R. Evans, The Interpretation of Small Molecule Diffusion Coefficients: Quantitative Use of Diffusion-Ordered NMR Spectroscopy, *Prog. Nucl. Magn. Reson. Spectrosc.*, 2020, **117**, 33–69, DOI: **10.1016/j.pnmrs.2019.11.002**.

23 D. Šmejkalová and A. Piccolo, Aggregation and Disaggregation of Humic Supramolecular Assemblies by NMR Diffusion Ordered Spectroscopy (DOSY-NMR), *Environ. Sci. Technol.*, 2008, **42**(3), 699–706, DOI: **10.1021/es071828p**.

24 See ESI† for details.